Fourth Asia-Pacific Conference on FRP in Structures (APFIS 2013)
11-13 December 2013, Melbourne, Australia

SIMPLE EQUATIONS OF SHEAR AND NORMAL STRESSES AT THE ENDS OF CFRP PLATE BONDED ONTO STEEL MEMBER

Masaru Shimizu [1], Toshiyuki Ishikawa [2], Atsushi Hattori [3] and Hirotaka Kawano [4]
[1] Department of Urban Management,
Kyoto University, Japan. Email: shimizu.masaru.75w@st.kyoto-u.ac.jp
[2] Department of Urban Management,
Kyoto University, Japan. Email: ishikawa.toshiyuki.2e@kyoto-u.ac.jp
[3] Department of Urban Management,
Kyoto University, Japan. Email: hattori.atsushi.7z@kyoto-u.ac.jp
[4] Department of Urban Management,
Kyoto University, Japan. Email: kawano.hirotaka.8n@kyoto-u.ac.jp

ABSTRACT

Recently, repair or strengthening of steel members by externally bonding Carbon Fiber Reinforced Polymer, CFRP, plate have been reported. While bonding CFRP plate can easily achieves increase in stiffness and strength, the debonding of CFRP plate from its ends is concerned. In Japan, the CFRP plates are also employed for enhancement of steel members with deterioration, fatigue cracks or low load-carrying capacity. Nevertheless, the verification method for debonding of CFRP plate has not been established. In this research, to encourage the development of verification method for debonding of CFRP plate, the differential equations of steel member with CFRP plate under typical load conditions, which are concentrated load and uniformly-distributed load, were derived and solved. As a result, the estimation equations of shear and normal stresses in adhesive at CFRP plate ends under typical load conditions were given. The shear and normal stresses at CFRP plate ends were provided as the functions of cross-sectional forces acting in the CFRP plate ends, regardless their distributions. Furthermore, the loading test on the cantilevered steel plate with bonded CFRP plate was conducted. Debonding strength from the test results was approximately evaluated with principal stress in the adhesive, which is calculated from the estimated shear and normal stresses proposed in this paper.

KEYWORDS

CFRP plate, steel member, debonding, shear stress, normal stress, principal stress

INTRODUCTION

For steel members with deterioration, fatique cracks or low load-carrying capacity, reinforcement with externally bonded CFRP plate has been widely reported (Miller *et al.* 2001;Moy and Bloodworth 2007 and Täljsten *et al.* 2009). Although the reinforcement by bonding CFRP plate can easily achieve increase in stiffness and strength, debonding of CFRP plate from the steel member is essentially concerning.
When traffic loads apply on the steel member strengthened with CFRP plate, shear and normal stresses occur into the adhesive layer, which are considered to encourage debonding failure. The shear and normal stresses in adhesive have been analysed theoretically or Finite Element (FE) analysis (Smith *et al*. 2001 and Deng *et al*. 2004). Theoretical solutions allow us to easily calculate the shear and normal stresses in adhesive layer while FE analysis often needs some effort to make analysis model. Thereby, some guidelines for strengthening steel member with CFRP plate employs the theoretical solution as a estimation method of the shear and normal stress in adhesive (Cadei *et al*. 2004; National Research Council 2007 and Schnerch *et al*. 2007a). However, the solution of shear and normal stresses heve been provided only for some specific conditions (National Research Council 2007 and Schnerch *et al*. 2007a). Therefore, engineers are required to derive the solutions for corresponding situations by themselves (Cadei *et al*. 2004).
Meanwhile, shear and normal stresses at the CFRP plate ends, where debonding of CFRP plate usually initiates, are the most important in design check for debonding. Therefore, this study mainly focuses on the shear and normal stresses at the CFRP plate ends. The equations for shear and normal stresses at CFRP plate ends were simplified in this paper. Furthermore, debonding test of cantilevered steel plate with bonded CFRP plate was conducted to evaluate the debonding strength by using proposed equations.

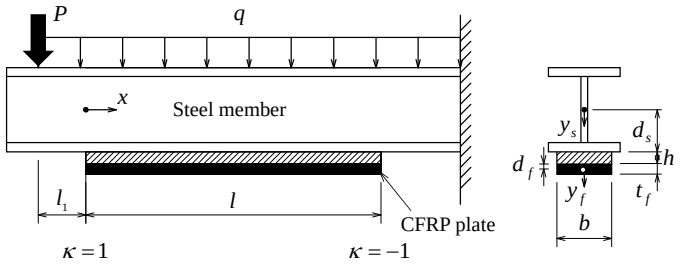

Figure 1 A cantilevered steel member with bonded CFRP plate subjected to a concentrated load and uniformly-distributed load (UDL)

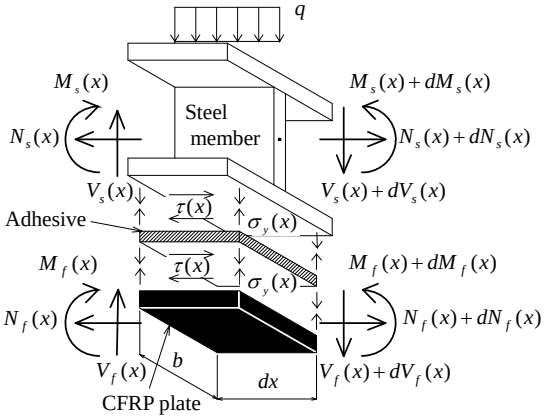

Figure 2 A differential segment of strengthened steel member

SHEAR AND NORMAL STRESSES IN ADHESIVE FOR A TYPICAL LOAD CONDITION

Differential Equations

In this section, the shear and normal stresses in the adhesive are theoretically derived under a typical load condition. During this analysis, the assumptions are: (1) materials are all linearly elastic, (2) the shear and normal stresses in adhesive layer are constant through the thickness, (3) the axial force, shear force and bending moment contributed by adhesive layer are negligible because of the low elasticity of the adhesive and relatively small cross-sectional area. These assumptions have been validated with Finite Element analysis in previous studies (Smith *et al*. 2001 and Deng *et al*. 2004).

A cantilevered steel member with bonded CFRP plate, as shown in Fig. 1, is used as the theoretical model. The internal forces acting on a differential segment in the strengthened section are shown in Fig. 2. From the equilibrium of the cross-sectional forces in the differential segment, the differential equations regarding the axial force and the shear force in the steel member, $N_s(x)$ and $V_s(x)$, are derived by (Ishikawa 2010):

$$\frac{d^2N_s(x)}{dx^2} - c^2 N_s(x) = c^2 \frac{K}{a} M(x) \tag{1}$$

$$\frac{d^4V_s(x)}{dx^4} + 4\omega^4 V_s(x) = \frac{4\omega^4}{Z_1}\left(Q(x) + J\frac{dN_s(x)}{dx}\right) \tag{2}$$

where $c = \sqrt{bG_e/h \cdot \left\{1/E_sA_s + 1/E_fA_f + a^2/\left(E_sI_s + E_fI_f\right)\right\}} = \sqrt{a^2bG_e/(hKZ_1E_sI_s)}$, $Z_1 = 1 + I_f/(nI_s)$, $Z_2 = 1 + nA_s/A_f$, $K = 1/(1 + Z_1Z_2r_s^2/a^2)$, $r_s = \sqrt{I_s/A_s}$, $a = d_s + d_f + h$, $\omega = \sqrt[4]{bE_eZ_1/(4hE_fI_f)}$, $n = E_s/E_f$, $J = d_f + (1 - Z_1)d_s + (1 - Z_1/2)h$, E_s is the elastic modulus of the steel, E_f is the elastic modulus of the CFRP plate, E_e is the elastic modulus of the adhesive, G_e is the shear modulus of the adhesive, A_s is the cross-sectional area of the steel member, A_f is the cross-sectional area of the CFRP plate, I_s is the moment of inertia of the steel member, I_f is the moment of inertia of the CFRP plate, d_s is the distance between the centroid of the steel member and its lower surface, d_f is the distance between the centroid of the CFRP plate and its upper surface, h is the thickness of the adhesive layer, b is the bond width of the adhered CFRP plate, $Q(x)$ is the shear force, $M(x)$ is the bending moment and x is the distance from the end of the CFRP plate, as illustrated in Fig. 2.

The general solutions of the axial force and shear force in the steel member, $N_s(x)$ and $V_s(x)$, are respectively given as:

$$N_s(x) = X_1 \sinh(cx) + X_2 \cosh(cx) - \frac{K}{a}\left\{M(x) + \frac{1}{c^2}\cdot\frac{d^2M(x)}{dx^2}\right\} \tag{3}$$

$$V_s(x) = Y_1 \cosh(\omega x)\sin(\omega x) + Y_2 \sinh(\omega x)\cos(\omega x) + Y_3 \cosh(\omega x)\cos(\omega x) + Y_4 \sinh(\omega x)\sin(\omega x) + W\left\{X_1 \cosh(cx) + X_2 \sinh(cx)\right\} + \frac{1}{Z_1}\left[\left\{1 - \frac{JK}{a}\right\}Q(x) + \frac{JK}{ac^2}\cdot\frac{d^3M(x)}{dx^3}\right] \tag{4}$$

where $W = 4/\left\{4 + (c/\omega)^4\right\}\cdot cJ/Z_1$, X_1 and X_2 are the unknown coefficients corresponding to the axial force in the steel member, Y_1 to Y_4 are the unknown coefficients corresponding to the shear force in the steel member.

From the equilibrium of the horizontal and vertical forces in the differential segment of the steel member, the shear and normal stresses in the adhesive, $\tau(x)$ and $\sigma_y(x)$, are given as:

$$\tau(x) = -\frac{1}{b}\cdot\frac{dN_s(x)}{dx} \tag{5}$$

$$\sigma_y(x) = -\frac{1}{b}\left\{\frac{dV_s(x)}{dx} + q\right\} \tag{6}$$

where q is the uniformly-distributed load (UDL).

Note from Eqs. (3) to (6), the shear and normal stresses in the adhesive involve unknown coefficients, which are determined from load conditions and boundary conditions.

The stresses in the steel member and CFRP plate, $\sigma_s(x)$ and $\sigma_f(x)$, introduced by the axial force and bending moment, are respectively given as:

$$\sigma_s(x) = \frac{N_s(x)}{A_s} + \frac{M_s(x)}{I_s}y_s \tag{7}$$

$$\sigma_f(x) = \frac{N_f(x)}{A_f} + \frac{M_f(x)}{I_f}y_f \tag{8}$$

where y_s is the distance from the centroid of the steel member, y_f is the distance from the centroid of the CFRP plate, $M_s(x)$ is the bending moment in the steel member, $N_f(x)$ is the axial force in the CFRP plate, $M_f(x)$ is the bending moment in the CFRP plate.

From the equilibrium of the horizontal forces, vertical forces and moments balance at x, the axial force, shear force and bending moment in the CFRP plate, $N_f(x)$, $V_f(x)$ and $M_f(x)$ are respectively given as:

$$N_f(x) = -N_s(x) \tag{9}$$

$$V_f(x) = Q(x) - V_s(x) \tag{10}$$

$$M_f(x) = M(x) - M_s(x) + N_s(x)a \tag{11}$$

The bending moment in the steel member, $M_s(x)$, is given as:

$$M_s(x) = \frac{1}{Z_1}\left\{M(x) + N_s(x)a\right\} - \frac{1}{4\omega^4}\cdot\frac{d^3V_s(x)}{dx^3} \tag{12}$$

Boundariy Conditions

For a cantilevered steel member with CFRP plate subjected to concentrated load and UDL, as illustrated in Fig. 1, the shear force and bending moment, $Q(x)$ and $M(x)$, is expressed as:

$$Q(x) = -P - q\left(x + l_1\right) \qquad (0 \le x \le l) \tag{13}$$

$$M(x) = -P(x + l_1) - \frac{q\left(x + l_1\right)^2}{2} \qquad (0 \le x \le l) \tag{14}$$

where P is the concentrated load, l_1 is the distance between the concentrated load and CFRP plate end, and l is the bond length of CFRP plate. The left end of UDL is corresponding to the concentrated load.

By applying the boundary conditions of $N_s(x=0) = 0$ and $N_s(x=l) = 0$ for Eq. (3), the unknown coefficients for the axial force in the steel member, X_1 and X_2, are given as:

$$X_1 = \frac{K}{a}\cdot\frac{1}{\sinh(cl)}\left[\left\{M(x=l) - \frac{q}{c^2}\right\} - \left\{M(x=0) - \frac{q}{c^2}\right\}\cosh(cl)\right] \tag{15}$$

$$X_2 = \frac{K}{a}\left\{M(x=0) - \frac{q}{c^2}\right\} \tag{16}$$

By applying the boundary conditions of $V_s(x=0)=-P-ql_1$, $V_s(x=l)=-P-q(l+l_1)$, $M_s(x=0)=-Pl_1-q{l_1}^2/2$, and $M_s(x=l)=-P(l+l_1)-q(l+l_1)^2/2$ for Eq. (4), the unknown coefficients for the shear force in the steel member, Y_1 to Y_4, are given as:

$$Y_1=\frac{1}{Z_3}\left[Z_5\left[\left(1-\frac{1}{Z_1}+\frac{JK}{aZ_1}\right)Q(x=l)-W\{X_1\cosh(cl)+X_2\sinh(cl)\}\right]\right.$$
$$-\frac{Z_3Z_6-Z_4Z_5}{2}\left\{\left(1-\frac{1}{Z_1}+\frac{JK}{aZ_1}\right)Q(x=0)-WX_1\right\}+2\omega\left(1-\frac{1}{Z_1}\right)\left\{M(x=l)-\frac{Z_3+Z_4}{2}M(x=0)\right\} \quad (17)$$
$$\left.+\frac{W}{2}\left(\frac{c}{\omega}\right)^3\left\{X_1\sinh(cl)+X_2\cosh(cl)-\frac{Z_3+Z_4}{2}X_2\right\}\right]$$

$$Y_2=\frac{1}{Z_3}\left[Z_5\left[\left(1-\frac{1}{Z_1}+\frac{JK}{aZ_1}\right)Q(x=l)-W\{X_1\cosh(cl)+X_2\sinh(cl)\}\right]\right.$$
$$-\frac{Z_3Z_6-Z_4Z_5}{2}\left\{\left(1-\frac{1}{Z_1}+\frac{JK}{aZ_1}\right)Q(x=0)-WX_1\right\}+2\omega\left(1-\frac{1}{Z_1}\right)\left\{M(x=l)-\frac{Z_4-Z_3}{2}M(x=0)\right\} \quad (18)$$
$$\left.+\frac{W}{2}\left(\frac{c}{\omega}\right)^3\left\{X_1\sinh(cl)+X_2\cosh(cl)-\frac{Z_4-Z_3}{2}X_2\right\}\right]$$

$$Y_3=\left(1-\frac{1}{Z_1}+\frac{JK}{aZ_1}\right)Q(x=0)-WX_1 \quad (19)$$

$$Y_4=\frac{1}{Z_3}\left[2\left[\left(1-\frac{1}{Z_1}+\frac{JK}{aZ_1}\right)Q(x=l)-W\{X_1\cosh(cl)+X_2\sinh(cl)\}\right]\right.$$
$$+Z_4\left\{\left(1-\frac{1}{Z_1}+\frac{JK}{aZ_1}\right)Q(x=0)-WX_1\right\}+2\omega\left(1-\frac{1}{Z_1}\right)\left\{-Z_6M(x=l)+\frac{Z_4Z_6-Z_3Z_5}{2}M(x=0)\right\} \quad (20)$$
$$\left.+\frac{W}{2}\left(\frac{c}{\omega}\right)^3\left[-\{X_1\sinh(cl)+X_2\cosh(cl)\}Z_6+\frac{Z_4Z_6-Z_3Z_5}{2}X_2\right]\right]$$

where $Z_3=\sinh(\omega l)/\sin(\omega l)-\sin(\omega l)/\sinh(\omega l)$, $Z_4=\sinh(\omega l)/\sin(\omega l)+\sin(\omega l)/\sinh(\omega l)$, $Z_5=1/\tan(\omega l)-1/\tanh(\omega l)$, $Z_6=1/\tan(\omega l)+1/\tanh(\omega l)$.

Shear and Normal Stresses in Adhesive Layer

From Eqs. (3) and (5), the shear stress in the adhesive layer is given as:

$$\tau(x)=-\frac{c}{b}\{X_1\cosh(cx)+X_2\sinh(cx)\}-\frac{K}{ab}\{P+q(x+l_1)\} \quad (21)$$

For a cantilevered steel member with bonded CFRP plate, as shown in Fig. 1, the distribution of shear stress in adhesive layer is shown in Fig. 3(a). The dimensions and material properties of specimens in debonding test, as mentioned below, are used. The distribution indicates that the maximum magnitude of shear stress occurs at the CFRP plate end near the fixed side of the steel member $x=300$mm.

As mentioned above, the shear stress in adhesive includes the unknown coefficient X_1 and X_2, determined by the load and boundary condintions. However, when a sufficiently long CFRP plate is bonded onto the steel

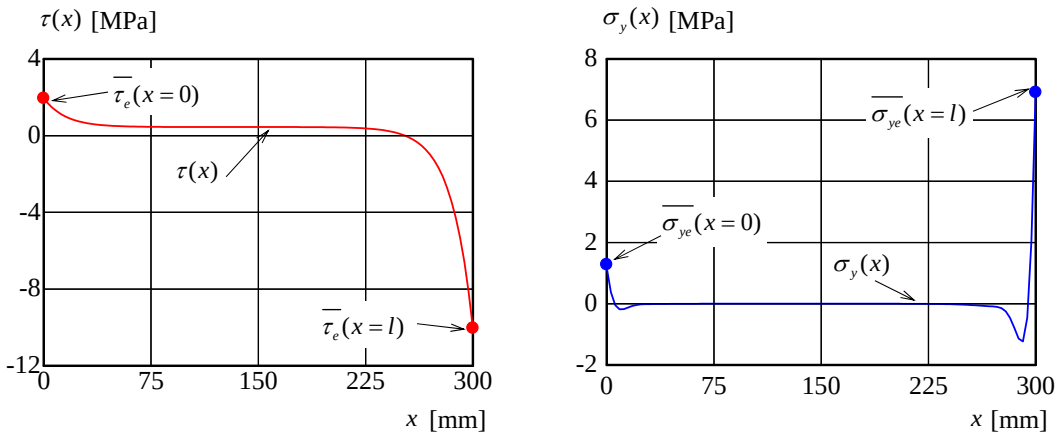

(a) Shear stress (b) Normal stress

Figure 3 Shear and normal stress in adhesive

member, the shear stresses at $x=0$ and $x=l$ respectively converge to:

$$\bar{\tau}(x=0)=\frac{cK}{ab}\left\{M(x=0)+\frac{1}{c}Q(x=0)-\frac{q}{c^2}\right\} \tag{22}$$

$$\bar{\tau}(x=l)=-\frac{cK}{ab}\left\{M(x=l)-\frac{1}{c}Q(x=l)-\frac{q}{c^2}\right\} \tag{23}$$

Note from Eqs. (22) and (23), the shear stress at the CFRP plate ends, $x=0$ and $x=l$, are simplified as function of cross-sectional forces at the CFRP plate ends. The fact implies the shear stresses at the CFRP plate ends can determine from the cross-sectional forces at the end of CFRP plates, regardless of its distributions. In addition, hyperbolic functions are not included in Eqs. (22) and (23). Therefore, Eqs. (22) and (23) enable us to estimate the shear stress at the CFRP plate end without divergence problem.

The convergent shear stresses, Eqs. (22) and (23), are plotted in Fig. 3(a). As can be seen from this figure, the convergent shear stresses given by Eqs. (22) and (23) are on the shear stress distribution ends.

From the tendency of components of Eqs. (22) and (23), the equations of shear stress at the end of CFRP plate can be simplified as:

$$\overline{\tau_e}=\kappa\frac{cK}{ab}\left(M_e+\frac{\kappa}{c}Q_e-\frac{q}{c^2}\right) \tag{24}$$

where $\overline{\tau_e}$ is the convergent shear stress at the end of CFRP plate, M_e and Q_e are the bending moment and shear force at the CFRP plate end, respectively, the value of κ is 1 for the left end of the CFRP plate and -1 for the right end of the CFRP plate, as shown in Fig. 1.

For I-shaped steel member, the value of Z_1 included in coefficient K can be regarded as 1 because the moment of inertia of the steel member is usually much larger than that of the CFRP plate. Consequently, the convergent shear stresses at the end of CFRP plate are rewritten as:

$$\overline{\tau_e}=\kappa\frac{c_0K_0}{ab}\left(M_e+\frac{\kappa}{c_0}Q_e-\frac{q}{{c_0}^2}\right) \tag{25}$$

where $c_0=\sqrt{a^2bG_e/(hK_0E_sI_s)}$ and $K_0=1/(1+Z_2r_s^2/a^2)$.

Meanwhile, from Eqs. (4) and (7), the normal stress in the adhesive is given as:

$$\begin{aligned}\sigma_y(x)=-\frac{\omega}{b}\big[&Y_1\{\sinh(\omega x)\sin(\omega x)+\cosh(\omega x)\cos(\omega x)\}+Y_2\{\cosh(\omega x)\cos(\omega x)-\sinh(\omega x)\sin(\omega x)\}\\&+Y_3\{\sinh(\omega x)\cos(\omega x)-\cosh(\omega x)\sin(\omega x)\}+Y_4\{\cosh(\omega x)\sin(\omega x)+\sinh(\omega x)\cos(\omega x)\}\big]\\&-\frac{cW}{b}\{X_1\sinh(cx)+X_2\cosh(cx)\}-\frac{q}{b}\left\{1-\frac{1}{Z_1}+\frac{JK}{aZ_1}\right\}\end{aligned} \tag{26}$$

For a cantilevered steel member with bonded CFRP plate, as shown in Fig. 1, the distribution of normal stress in adhesive layer is shown in Fig. 3(b). Similar to the shear stress in the adhesive, stress concentration also occurs at the adhesive ends. In addition, the maximum compressive normal stress occurs at the CFRP plate end near the fixed side of the steel member $x=300$mm.

If a sufficiently long CFRP plate is bonded onto the lower surface of the steel member, the normal stresses at $x=0$ and $x=l$, respectively, converge to:

$$\begin{aligned}\overline{\sigma_y}(x=0)=\frac{\omega}{b}\Bigg[&W\frac{K}{a}\left\{2+\frac{1}{2}\left(\frac{c}{\omega}\right)^3-\frac{c}{\omega}\right\}\left\{M(x=0)-\frac{q}{c^2}\right\}+2\omega\left(1-\frac{1}{Z_1}\right)M(x=0)\\&+2\left(1-\frac{1}{Z_1}+\frac{JK}{aZ_1}\right)Q(x=0)-\left(1-\frac{1}{Z_1}+\frac{JK}{aZ_1}\right)\frac{q}{\omega}\Bigg]\end{aligned} \tag{27}$$

$$\begin{aligned}\overline{\sigma_y}(x=l)=\frac{\omega}{b}\Bigg[&W\frac{K}{a}\left\{2+\frac{1}{2}\left(\frac{c}{\omega}\right)^3-\frac{c}{\omega}\right\}\left\{M(x=l)-\frac{q}{c^2}\right\}+2\omega\left(1-\frac{1}{Z_1}\right)M(x=l)\\&-2\left(1-\frac{1}{Z_1}+\frac{JK}{aZ_1}\right)Q(x=l)-\left(1-\frac{1}{Z_1}+\frac{JK}{aZ_1}\right)\frac{q}{\omega}\Bigg]\end{aligned} \tag{28}$$

Note from Eqs. (27) and (28), similarly to the shear stress at the CFRP plate ends, the normal stress at the CFRP plate ends, $x=0$ and $x=l$, are simplified as function of cross-sectional forces at the CFRP plate ends. Therefore, both shear and normal stresses at the CFRP plate ends are determined from cross-sectional forces at the CFRP plate ends, regardless of their distributions and boundary condition.

The convergent normal stresses, Eqs. (27) and (28), are plotted in Fig. 3(b). As can be seen from this figure, the convergent normal stresses, given by Eqs. (27) and (28), are on the ends of the normal stress distribution.

From the tendency of the components of Eqs. (27) and (28), they can be simplified as:

$$\overline{\sigma_{ye}} = \frac{\omega}{b}\left[W\frac{K}{a}\left\{2+\frac{1}{2}\left(\frac{c}{\omega}\right)^3-\frac{c}{\omega}\right\}\left\{M_e-\frac{q}{c^2}\right\}+2\omega\left(1-\frac{1}{Z_1}\right)M_e \right.$$
$$\left. +2\kappa\left(1-\frac{1}{Z_1}+\frac{JK}{aZ_1}\right)Q_e-\left(1-\frac{1}{Z_1}+\frac{JK}{aZ_1}\right)\frac{q}{\omega}\right] \quad (29)$$

where $\overline{\sigma_{ye}}$ is the convergent normal stress at the ends of CFRP plate.
For I-shaped steel member, the value of Z_1 can be regarded as 1. Further, the values of $(c/\omega)^3$ and $(c/\omega)^4$ can be regarded as 0, because they are negligibly-small. Consequently, the equations for the convergent normal stresses at $x=0$ and $x=l$ are rewritten as:

$$\overline{\sigma_{ye}} = \frac{c_0\omega_0 d_f K_0}{ab}\left\{\left(2-\frac{c_0}{\omega_0}+\frac{2a}{d_f K_0}\cdot\frac{\omega_0}{c_0}\cdot\frac{I_f}{nI_s}\right)M_e+\kappa\frac{2}{c_0}Q_e-\frac{2}{c_0^{\,2}}q\right\} \quad (30)$$

where $\omega_0 = \sqrt[4]{bE_e/(4hE_f I_f)}$.
In Eq. (30), a coefficient of bending moment, I_f/nI_s, is exceptionally remained to enhance the precision of convergent normal stresses.

EVALUATION OF DEBONDING FAILURE BY PROPOSED EQUATIONS

Debonding Test

To evaluate the debonding strength by proposed equation, loading test for cantilevered steel plate with bonded CFRP plate is carried out. Figure 4 shows the test-setup. The CFRP plates were bonded onto the lower or the upper surface of the steel plate with two component epoxy resin. One end of the steel plate is fixed to a rigid frame and a concentrated load was applied on the other end of steel plate by using mechanical jack. Strain gauges are placed on the steel plate and CFRP plate at the distance of 5 and 20mm from the end of CFRP plate and its centre, as illustrated in Fig. 5. The strain gage at 5mm from the CFRP plate end is used to detect the debonding. To check the yield strain of steel plate, the strain in unstrengthened section was also measured.

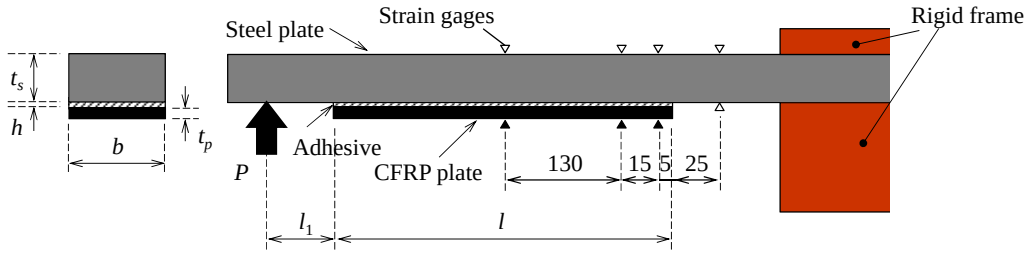

Figure 4 Test set-up

Table 1 Test specimens and results

Specimen	Adhesive thickness [mm]	Debonding load [kN]	Convergent shear stress [MPa]	Convergent normal stress [MPa]	Principal stress [MPa]	Mises stress [MPa]
T-1	0.85	0.45	-15.9	11.1	22.4	29.7
T-2	0.85	0.38	-13.4	9.34	18.9	25.0
T-3	1.15	0.36	-11.0	7.36	15.3	20.5
T-4	1.05	0.42	-13.4	9.08	18.7	24.9
T-5	1.05	0.36	-11.5	7.78	16.0	21.4
T-6	0.85	0.48	-16.9	11.8	23.8	31.6
Average	0.97	0.41	-13.7	9.40	19.2	25.5
C-1	0.75	0.9	33.7	-23.9	23.8	63.1
C-2	0.75	0.88	33.0	-23.3	23.3	61.7
C-3	0.8	0.88	32.0	-22.4	22.7	59.8
C-4	0.93	1.14	38.6	-26.5	27.5	71.9
C-5	0.90	1.04	35.7	-24.7	25.5	66.6
Average	0.83	0.97	34.6	-24.2	24.6	64.6
Average of all data	0.90	—	—	—	21.6	43.3

Table 2 Dimensions and material properties of test specimens

(a) Steel plate

Width × thickness [mm]	50 × 11.6
Location of load: l_1 [mm]	50
Elastic modulus: E_s [GPa]	202

(b) CFRP plate

Width: b × thickness: t_f [mm]	50 × 2.7
Length: l [mm]	300
Elastic modulus: E_f [GPa]	332

(c) Adhesive

Thickness: h [mm]	0.9
Elastic modulus: E_e [GPa]	2.6
Shear modulus: G_e [GPa]	1.0

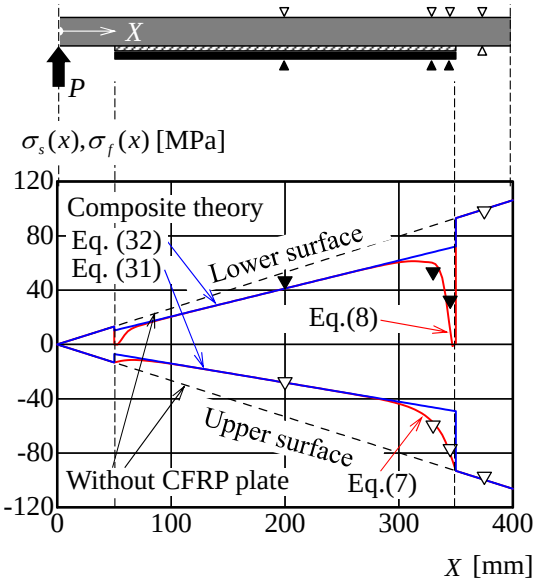

Figure 5 Stress distributions of steel member and CFPR plate

The specimens are all listed in Table 1. In this table, the label 'T' denotes the specimens with the CFRP plate in its tension side and the label 'C' denotes the specimens with the CFRP plate in its compression side. The adhesive thicknesses measured from the specimens are also listed in Table 1.
For the steel plate, thickness of 11.6mm, width of 50mm and elastic modulus of 202 GPa were used. The CFRP plate with thickness of 2.7mm, width of 50mm and elastic modulus of 332 GPa was used. Dimensions and material properties used in this study are listed in Table 2.

Stresses in Steel and CFRP Plate

The stress in the steel and CFRP plate at the load of $P=-298$N are plotted on Fig. 5. Additionally, their stress distributions calculated from the Eqs.(7) and (8) are also described in Fig. 5. For comparison, their stress distributions based on the composite theory are also includes as:

$$\sigma_s(x)=\frac{M(x)}{I_v}y_v \tag{31}$$

$$\sigma_f(x)=\frac{M(x)}{nI_v}y_v \tag{32}$$

where I_v is the equivalent moment of inertia of the steel-CFRP composite member and y_v is the distance from the centroid of the steel-CFRP composite member.
As can be seen from the Fig. 5, Eqs. (7) and (8) closely demonstrate stress distributions of steel and CFRP plate. At the center of the CFRP plate, the stress in the steel member in its tension surface is reduced until that given by the composite theory. However, the stress in the steel member in the vicinity of CFRP plate ends is not sufficiently reduced to the composite theory due to shear-transfer lag effect caused by the adhesive layer.

Debonding Load and Convergent Shear and Normal Stresses in Adhesive

In all specimens, the debonding of CFRP plate was observed under the yield load of the steel plate. Debonding of CFRP plate occurred at the CFRP plate end near the fixed side and was detected by the strain measured at the distance of 5mm from the CFRP plate end. Figure 6 shows the relationship between applied load and strain obtained from the test. The relationship between load and strain shows the linearity until debonding of CFRP plate occurs. When the debonding of CFRP plate occurs, the strain at 5mm from the CFRP plate end significantly reduced. In this study, the load when the peak strain was recorded is defined as the debonding load P_d. Debonding loads P_d for all specimens are also listed in Table 1.
The series of specimens-C, for which the CFRP plate is bonded onto the compression side of steel plate, obviously higher debonding load than the series of specimens-T, for which the CFRP plate is bonded onto the tension side of steel plate.

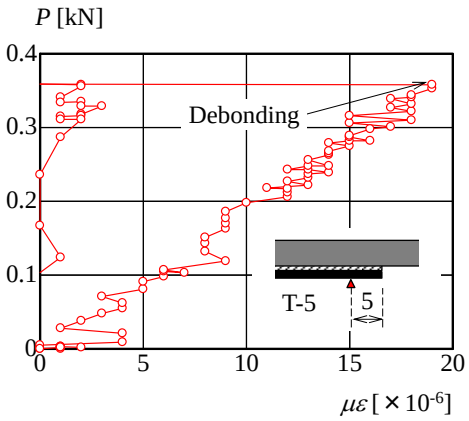

Figure 6 Relationship between applied load and strain at the distance of 5mm from the CFRP plate end

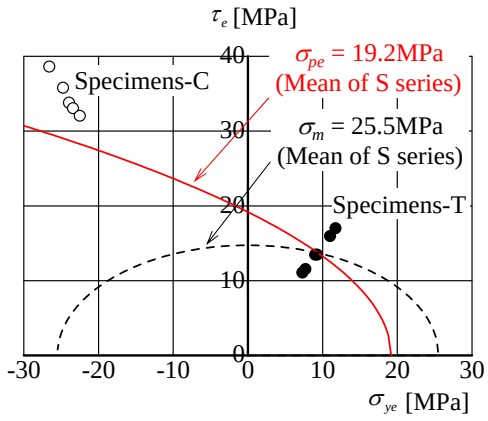

Figure 7 Relationship between shear and normal stress when debonding

Convergent shear and normal stresses at the end of CFRP plate calculated from Eqs.(24) and (29) with the debonding load are also listed in Table 1.
For the specimens-C, with the CFRP plate in its compression side, the normal stresses are negative and magnitudes of shear stresses of the specimens-C are obviously higher than that of the specimens-S.

Evaluation of bond strength

To verify the safety for debonding of CFRP plate, the principal stress in adhesive is often used (National Research Council 2007; Schnerch *et al*. 2007a and b). The principal stress in adhesive at the CFRP plate ends σ_{pe} is expressed as:

$$\sigma_{pe} = \frac{\overline{\sigma_{ye}}}{2} + \sqrt{\left(\frac{\overline{\sigma_{ye}}}{2}\right)^2 + \overline{\tau_e}^2} \tag{33}$$

The principal stresses in adhesive at the CFRP plate end for each specimen are listed in Table 1.
To evaluate the bond strength of tested specimens, the failure envelope based on the principal stress for 19.2MPa, the average of the principal stress of specimens-T, is described in Fig.7 as a solid line. For comparison, the failure envelope based on the von-Mises stress in adhesive σ_{me}, as calculated in the following equation, given by the test results of specimens-T is also drawn in Fig. 7 as a dashed line:

$$\sigma_{me} = \sqrt{\sigma_{ye}^2 + 3\tau_e^2} \tag{34}$$

It can be seen from the negative region of normal stress in Fig. 7, the failure envelope based on the principal stress shows the different tendency from the failure envelope based on von-Mises stress.
For the failure envelope based on the principal stress, shear stress in negative region of normal stress is higher than that in positive region of normal stress. Although the failure envelope is given from the average of the principal stress of specimens-T, the failure envelope also approximately demonstrates the test results of specimens-C.
By contrast, the failure envelope based on von-Mises stress is symmetric about the y-axis. Disagreement between the failure envelope based on von-Mises stress and test results of the specimens-C can be seen. Thus, the reliability for prediction of bond strength based on von-Mises stress depends on the bonding condition of CFRP plate.

CONCLUSIONS

To encourage the development of verification method for debonding of CFRP plate, simple equations for shear and normal stresses at the CFRP plate ends were derived. Furthermore, evaluation of test results using proposed equation was conducted. Findings are followings:

(1) Focusing on the shear and normal stress at the CFRP plate ends, their stresses were simply expressed as the functions of cross-sectional forces acting on CFRP plate ends. The equations for shear and normal stresses included no hyperbolic functions.
(2) Debonding loads of the specimens with CFRP plate in its tension side and compression side were significantly difference. However, their principal stress, calculated from proposed shear and normal stresses in adhesive, were approximately the same magnitude. Therefore, the debonding strength can be predicted by using the principal stress based criterion.

ACKNOWLEDGEMENTS

The authors grateful acknowledge the financial support provided by JSPS Grant-in-Aid for challenging Exploratory Research (24656269).

REFERENCES

Cadei J.M.C., Strafford T.J., Hollaway L.C. and Duckett W.G. (2004). "Strengthening Metallic Structures Using Externally Bonded Fibre-Reinforced Polymers", CIRIA 2004, ISBN 0-86017-595-2.

Deng J., Lee M.M.K. and Moy S.S.J. (2004) "Stress analysis of steel steel members reinforced with a bonded CFRP plate", *Composite Structures*, Vol.65, 205-215.

Ishikawa T. (2010) "Debonding bending moment of pre-stressed CFRP bonded steel member", *Journal of Structural Engineering A*, Vol. 56A, 991-998. (in Japanese)

Miller T.C., Chajes M.J., Mertz D.R. and Hastings J.N. (2001) "Strengthening of a Steel Bridge Girder Using CFRP Plates", *Journal of Bridge Engineering*, ASCE, USA, Vol.6, 514-522.

Moy, S.S.J. and Bloodworth, A.G. (2007). "Strengthening a steel bridge with CFRP composites", *Proceedings of the Institution of Civil Engineers*, Structures & Buildings 160, Issue SB2, 81-93.

National Research Council. Advisory Committee on Technical Recommendations for Construction (2007). "Guidelines for the Design and Construction of Externally Bonded FRP Systems for Strengthening Existing Structures", CNR-DT 202/2005.

Smith S.T. and Teng J.G. (2001) "Interfacial stresses in plated steel members", *Engineering Structures*, Vol.23, 857-871.

Schnerch D., Dawood M., Rizkalla S. and Sumner E. (2007a). "Design Guidelines for the Use of HM Strips: Strengthening of Steel Concrete Composite Bridges with High Modulus Carbon Fiber Reinforced Polymer (CFRP) Strips", NC State University Technical Report, No. IS-06-02.

Schnerch D., Dawood M., Rizkalla S. and Sumner E. (2007b). "Proposed design Guidelines for strengthening of steel bridges with FRP materials", Construction and Building Materials 21, 1001-1010.

Täljsten B., Hansen C.S. and Schmidt J.W. (2009) Strengthening of old metallic structures in fatigue with prestressed and non-prestressed CFRP laminates, *Construction and Building Materials*, Vol.23, 1665–1677.